Kinetics of photocatalytic degradation of diuron in aqueous colloidal solutions of Q-TiO$_2$ particles

Kateřina Macounová[*], Hana Krýsová, Jiří Ludvík, Jaromír Jirkovský

J. Heyrovský Institute of Physical Chemistry, Academy of Sciences of the Czech Republic, Dolejškova 3, 182 23 Prague 8, Czech Republic

Abstract

Kinetics of the photocatalytic degradation of a phenylurea herbicide diuron in aqueous colloidal solutions of Q-TiO$_2$ nanoparticles was analyzed in detail applying a model of parallel consecutive reactions of the first-order. The found mechanism was compared with the reaction pathways of electrochemically assisted photoprocesses on illuminated TiO$_2$ layers, polarized by external voltage, in various solvents. While a reductive dechlorination on benzene ring of diuron represented the major pathway in acetonitrile, a consecutive oxidative demethylation on the aliphatic side chain was mainly observed in water.
© 2003 Published by Elsevier Science B.V.

Keywords: Photocatalytic degradation; Phenylurea herbicide diuron; Q-TiO$_2$ particles

1. Introduction

Diuron [3-(3,4-dichlorophenyl)-1,1-dimethylurea] belongs to halogenophenylureas representing an important class of contact herbicides that have been used worldwide for more than 40 years. Their specific effect consists in an inhibition of photosynthetic electron transport of germinating grass and broad-leaved weeds in many crops. Due to low solubility and chemical stability of halogenophenylureas, they penetrate slowly through soil and contaminate underground sources of drinking water. Their photoreactivity has been already studied several times [1]. Chloranilines as their possible degradation intermediates are toxic compounds pretending an additional risk. Two different transformation pathways are typical for photodegradation of halogenophenylureas. They react either on the aromatic ring or on the side urea chain.

In the paper of Jirkovský et al. [2], a direct photolysis of diuron was studied under various conditions. In aqueous conditions, a substitution of chlorine atoms by hydroxyl groups was observed. Proportion between two isomeric products depended on the irradiation wavelength: 3-(4-chloro-3-hydroxyphenyl)-1,1-dimethylurea was mainly formed applying shorter irradiation wavelengths (λ < 310 nm) while 3-(3-chloro-4-hydroxyphenyl)-1,1-dimethylurea predominated using longer wavelengths (λ > 310 nm).

On the other hand, if dispersed on dry quartz sand and other solid surfaces, diuron underwent demethylation. First 3-(3,4-dichlorophenyl)-1-formyl-1-methylurea and 3-(3,4-dichlorophenyl)-1-methylurea were formed. The latter compound was then phototransformed via 3-(3,4-dichlorophenyl)-1-formyl urea to 3,4-dichlorophenyl urea. The reductive dechlorination of the benzene ring was observed as a minor reaction pathway under these conditions.

The reductive dechloration was also described for monuron [3-(4-chlorophenyl)-1,1-dimethylurea] that was irradiated monochromatically at 256 nm in the presence of methanol [3]. The reaction led to fenuron [3-phenyl-1,1-dimethylurea].

A photoinduced degradation of diuron on its side chain taking place in aqueous solution of iron(III) perchlorate was studied by Mazellier et al. [4]. 3-(3,4-Dichlorophenyl)-1-formyl-1-methylurea was identified as a major primary intermediate. The suggested mechanism involves an attack of hydroxyl radical photogenerated upon excitation of iron(III) hydroxo complexes. Photocatalytic degradation of diuron employing TiO$_2$ as another source of the reactive hydroxyl radical was studied by Krýsová et al. [5]. They used a batch mode photoreactor with thin aqueous film circulating over immobilized TiO$_2$ layer irradiated by sun bed lamps (300–400 nm). Even here, a consecutive demethylation on the side aliphatic chain was the main observed process of the diuron transformation.

Photocatalysts based on TiO$_2$ are promising materials for water decontamination. Many organic substances have been

---

* Corresponding author.
E-mail address: katerina.macounova@jh-inst.cas.cz (K. Macounová).

mineralized to CO_2, H_2O and corresponding mineral acids using TiO_2 under irradiation [6]. The processes of photocatalytic degradation are induced by absorption of photons by semiconductor particles causing photogeneration of separated charge carriers. The positive holes can be trapped by surface hydroxyl groups forming highly reactive hydroxyl radicals. These highly oxidizing species react rapidly with almost every organic molecule and thus initiate its oxidative decomposition. The electrons are typically transferred to dioxygen yielding superoxide radical anion ($^\bullet O_2{}^-$). The dissolved dioxygen is an essential reaction component of the photocatalysis participating also in further steps of degradation. It can also repeatedly react with organic radicals originated from the primary OH-attacks leading to peroxyl radicals of various structures. These open-shell transients are usually transformed into corresponding close-shell organic molecules in higher oxidation states. There are two typical ways of these transformations: an elimination of hydroperoxyl radical ($^\bullet OOH$) and a bimolecular recombination of two peroxyl radicals. In the latter case, the initially formed tetraoxides represent unstable intermediates that usually decompose producing two oxygen-containing compounds. The repetition of these processes leads to gradual oxidation of the original organic compound, finally up to CO_2 as a substance with the highest oxidation level of carbon.

In this study, extremely small particles of titanium dioxide that exhibited a quantum size effect [7,8] were used (Q-TiO_2). Their physico-chemical properties depended on the particle dimension. Comparing to macroscopic TiO_2 powder materials, these particles showed a blue shift in their absorption spectra due to broadening of the band gap. Their aqueous dispersions do not practically scatter light. Therefore, the absorption spectroscopy including time-resolved methods can be employed to investigate the physico-chemical characteristics of Q-TiO_2 particles and also to measure the precise values of quantum yields of photocatalytic transformations occurring in their aqueous colloidal solutions.

In this paper, a detailed kinetic study of the photocatalytic degradation of diuron in aqueous colloidal solutions of the Q-TiO_2 particles is described. The corresponding reaction mechanism is compared with the pathways of electrochemically assisted photocatalytic transformation of diuron on irradiated TiO_2 layers polarized by external voltage in both aqueous and non-aqueous solvents.

2. Experimental

2.1. Preparation of Q-TiO_2

Colloidal solutions of the Q-TiO_2 particles were prepared by hydrolysis of titanium tetrachloride. A volume of 3.5 ml of $TiCl_4$ was slowly dropped into 900 ml of distilled water cooled to $1\,^\circ C$ under vigorous magnetic stirring. The formed colloidal solution was dialyzed against water to decrease
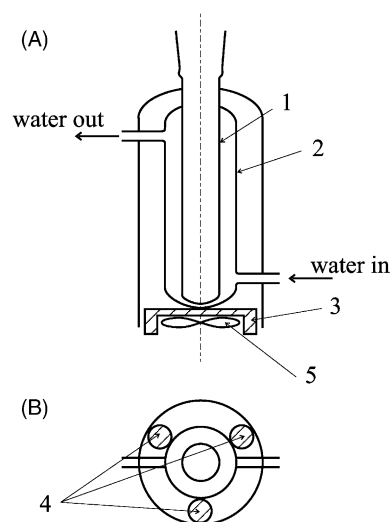

Fig. 1. The schematic picture of the tube photoreactor: (1) inner glass tube, (2) outer glass tube, (3) magnetic stirrer, (4) medium pressure mercury lamps, (5) ventilator.

its ionic strength. The dialysis was stopped after a pH of 2.5 was reached. Such colloidal solutions were stable for many months if kept at $4\,^\circ C$. The synthesized Q-TiO_2 particles were of 2–3 nm in diameter and possessed a crystalline structure of anatase [9].
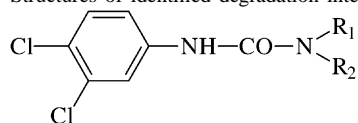
2.2. Photoreactor

A photoreactor designed and developed in our laboratory consisted of two coaxial quartz tubes placed in the axis of a metallic cylinder (Fig. 1). An inner tube (1) was filled by a volume of 70 ml of the reaction mixture that was continuously mixed by a magnetic stirrer (3) during the whole irradiation experiments. Cooling distilled water circulated in the space between the inner and outer tube (2) and its temperature was adjusted to $20\,^\circ C$. Three medium pressure mercury lamps (4) (RVU, 125 W, Tesla Holešovice, Czech Republic), symmetrically placed around the outer quartz tube, were used as a source of UV irradiation ($\lambda = 365$ nm). A ventilator (5) helping to cool the space inside the photoreactor was placed at the bottom of the photoreactor.

The incident light entering into the photoreactor was estimated by potassium ferrioxalate actinometry [15].

2.3. Photoelectrochemical cell

A detailed description of the used photoelectrochemical cell could be found in the paper [10]. A three-electrode arrangement consisted of Ag wire and Pt gauze as reference and counter electrodes, respectively. A thin TiO_2 layer prepared on Ti plate (22×40 mm^2) mounted in teflon holder served as a working electrode. The TiO_2 layer was deposited by spreading of a film of viscous dispersion [11] of TiO_2 particles [12] followed by heating at a temperature between

Table 1

Structures of identified degradation intermediates of diuron

Symbol	R_1	R_2	Chemical name	Characterization
D	CH_3	CH_3	3-(3,4-Dichlorophenyl)-1,1-dimethylurea	Diuron (starting compound)
I	CHO	CH_3	3-(3,4-Dichlorophenyl)-1-formyl-1-methylurea	Primary product
II	CH_2OH	CH_3	3-(3,4-Dichlorophenyl)-1-hydroxymethyl-1-methylurea	Primary product
III	H	CH_3	3-(3,4-Dichlorophenyl)-1-methylurea	Secondary product
IV	H	CHO	3-(3,4-Dichlorophenyl)-1-formylurea	Tertiary product
V	H	CH_2OH	3-(3,4-Dichlorophenyl)-1-hydroxymethylurea	Tertiary product[a]
VI	H	H	3,4-Dichlorophenylurea	Quarternary product

[a] The structure of this product **V** was assumed in analogy with the product **II**.

450 and 500 °C. The electrochemically assisted photocatalytic degradation of diuron on this TiO_2 layer was studied under both aqueous and non-aqueous conditions. The concentration of diuron was 5×10^{-5} mol l^{-1} in both cases. Acetonitrile containing 0.5 M $(CH_3CH_2CH_2)_4NBF_4$ was used as a solvent for non-aqueous experiments. The concentration changes of diuron were followed by HPLC.

2.4. Procedures and analytical techniques

The chromatographic analyses were performed on a Merck Hitachi HPLC set consisted of an absorption detector (L-4250) and an integrator (D-2500). The volume of an injection loop was 20 μl. A chromatographic column (LiChrospher® 100, RP-18, 5 μm) together with a guard column (LiChroCART® 4-4, RP-18, 5 μm) were used. A mixture of methanol and water (both in purity for HPLC) in a ratio of 7:3 was employed as a mobile phase. A flow rate of 1 ml min^{-1} was applied and a detection wavelength of 250 nm was adjusted. The retention time of diuron was about 6 min under these conditions.

The same chromatographic technique was also used to isolate the main degradation intermediates. The irradiated reaction mixture was extracted by ether. The extract was concentrated by evaporation and then repeatedly injected into HPLC. Particular fractions containing the main reaction components were collected. After evaporating solvent, they were identified employing MS and NMR techniques.

2.5. Identification of degradation intermediates

Following characteristic masses of molecular peaks were found in MS spectra of the particular degradation intermediates (Table 1):

I	246 (2Cl)	$C_9H_8O_2N_2Cl_2$
II	248 (2Cl)	$C_9H_{10}O_2N_2Cl_2$
III	218 (2Cl)	$C_8H_8ON_2Cl_2$
IV	232 (2Cl)	$C_8H_6O_2N_2Cl_2$
VI	204 (2Cl)	$C_7H_6ON_2Cl_2$

Characteristics of ^1H NMR spectra in CD_3OD are given in Table 2.

3. Results and discussion

3.1. Detailed reaction mechanism of the photocatalytic degradation of diuron on Q-TiO$_2$

On the bases of the identified reaction intermediates, the following reaction pathway for the photocatalytic degradation of diuron in colloidal solutions of the Q-TiO$_2$ particles was proposed.

The hydroxyl radical (OH$^\bullet$) photogenerated on the surface of the irradiated semiconductor particles reacts with one methyl group on the aliphatic side chain of diuron (**D**) under an abstraction of hydrogen atom. As a result, radical **R$_1$**$^\bullet$ is produced (1):
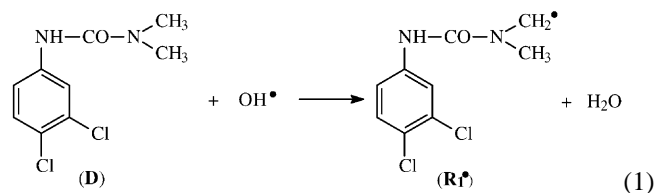

$$(1)$$

Table 2

Characteristics of ^1H NMR spectra of degradation intermediates of diuron measured in CD_3OD

I	7.910 d(1H)	7.540 d(1H)	7.400 dd(1H)		3.50 (CHD$_2$OD)
III	7.710 d(1H)	7.335 d(1H)	7.205 dd(1H)	3.12 s(3H)	3.50 (CHD$_2$OD)
IV	7.920 d(1H)	7.555 d(1H)	7.420 dd(1H)		3.50 (CHD$_2$OD)
VI	7.930 d(1H)	7.550 d(1H)	7.420 dd(1H)		3.50 (CHD$_2$OD)

In the presence of air dissolved in the solution, the radical $R_1^\bullet$ reacts preferentially with dioxygen yielding a peroxyl radical $R_1OO^\bullet$ (2). Its disproportionation, passing probably through a tetraoxide transient, leads to two main primary intermediates **I** and **II** (3):

(2)

(3)
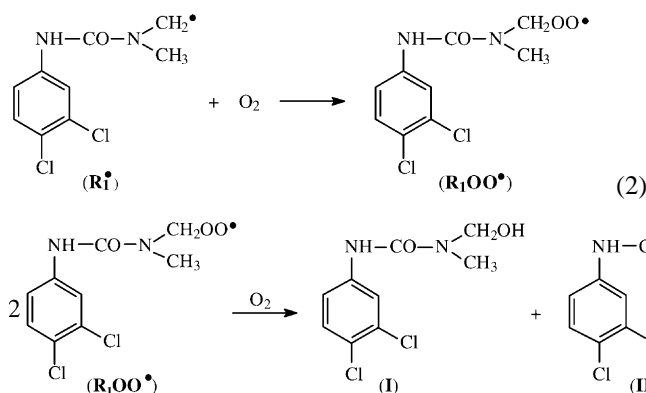
The compounds **I** and **II** were found to be thermally unstable, especially in acidic solutions ((4) and (5)). Both reactions, decomposition of **I** and hydrolysis of **II,** provided the same substance **III** as a secondary degradation intermediate. Dependence of the reaction rates of these processes on both temperature and pH was investigated.

(4)

(5)
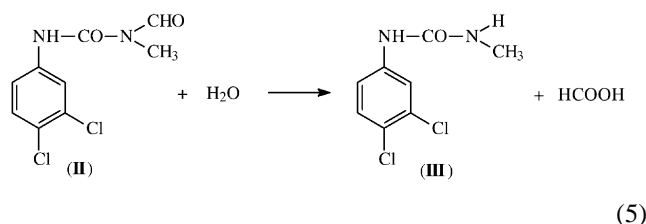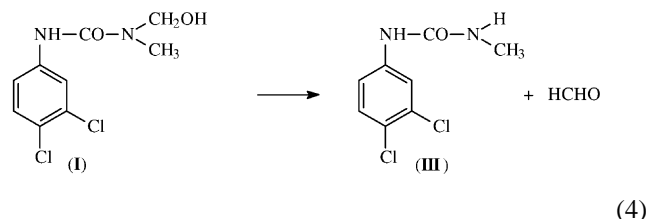
Analogously to starting diuron, a OH-attack on the remaining methyl group of the compound **III** initiates its parallel transformation to the tertiary intermediates **IV** and **V** with formyl and hydroxymethyl group on the side chain, respectively. Their thermal transformations lead to the compound **VI** as a quarternary degradation intermediate of diuron. The corresponding reaction scheme is proposed in Fig. 2.

3.2. Kinetic analysis of the diuron degradation in Q-TiO$_2$ colloidal solutions

It seems to be rather complicated to formulate a kinetic model that would describe all particular reactions mentioned above. However, it is possible to assume certain simplifications.

For a stable light intensity and non-changing properties of the Q-TiO$_2$ particles, the reaction rate of formation of hydroxyl radical is supposed to be constant during the whole photocatalytic experiment. In addition, this photogeneration of hydroxyl radical and the following OH-attack onto an organic molecule should represent a crucial step that controls the reaction rate of particular transformations of this molecule to its corresponding oxidized intermediates, e.g. $D \rightarrow I$ and $D \rightarrow II$ or $III \rightarrow IV$ and $III \rightarrow V$. If only unimolecular transformations such as an oxidation and decarboxylation occur during the photocatalytic degradation processes, the overall molar concentration of the organic substances present in the reaction system will remain constant. If the overall rate constants of OH-attacks on the starting organic compound and on its degradation intermediates are similar, an average reaction rate of the disappearance of hydroxyl radical should stay practically the same. Due to the non-changing reaction rates of photogeneration and consumption of hydroxyl radicals, their photostationary concentration have to remain approximately constant. In this consequence, the starting organic compound should disappear according to the first-order kinetics:

$$-\frac{d[D]}{dt} = k[OH^\bullet][D] = a_0[D] \qquad (6)$$

The formal pseudomonomolecular rate constant a_0 represents a product of the overall rate constant of the second kinetic order summing contributions of all occurring intermolecular reactions of hydroxyl radical with the starting organic compound (usually in the range 10^9–10^{10} l mol^{-1} s^{-1}) multiplied by the photostationary concentration of hydroxyl radical. Provided that this concentration is changing, the photocatalytic degradation of the starting compound would not be pseudomonomolecular. Therefore, a kinetic analysis of the experimental dependence of concentration of the starting compound on irradiation time will represent an important test. Any systematic deviation from the first-order kinetics would mean that some of the assumptions mentioned above were not fulfilled.

3.2.1. Influence of various parameters on the reaction rate of diuron

The course of photodegradation of diuron was studied as a function of various parameters such as light intensity, initial concentration of diuron, pH and concentration of Q-TiO$_2$ particles. In all cases, a pseudomonomolecular kinetics of the diuron disappearance during the whole irradiation experiment was observed. Three typical experimental dependences of the diuron concentration on irradiation time are shown
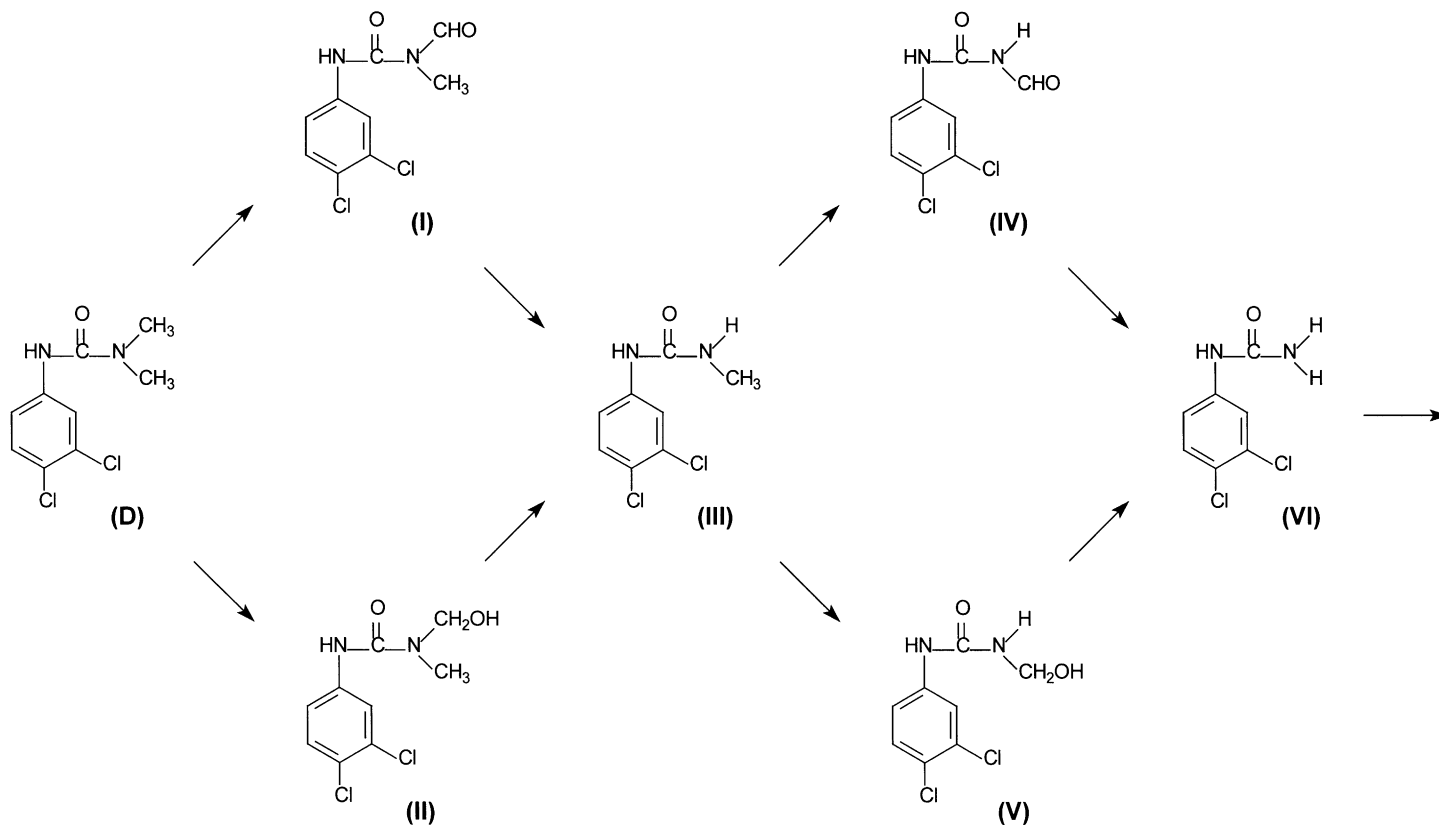
Fig. 2. The proposed reaction scheme of the photocatalytic degradation of diuron in aqueous colloidal solutions of Q-TiO$_2$ particles.
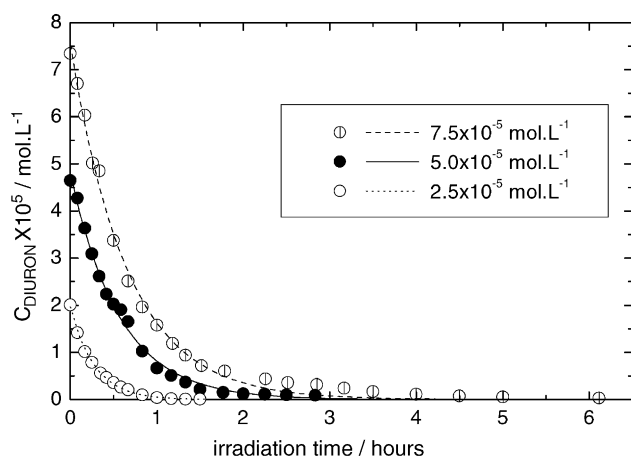
Fig. 3. The kinetic dependences of the photocatalytic degradation of diuron for its various starting concentration. Experimental conditions: 2×10^{-2} mol l^{-1} HClO$_4$, 10^{-3} mol l^{-1} Q-TiO$_2$, temperature 20 °C, one lamp.

in Fig. 3 together with the corresponding fits calculated according to the first-order kinetics. This fact confirms that the assumptions mentioned in the previous paragraph were correct and gave explanation for the observed pseudomonomolecular kinetics of the photocatalytic degradation of diuron in Q-TiO$_2$ colloidal solutions.

The formal first-order rate constants (a_0) of all experiments are listed in Table 3. The values of quantum yields (Φ), calculated on the bases of determined numbers of photons absorbed by the photocatalysts, are also included.

It can be seen from these data that the rate formal constants a_0 decreased while quantum yields Φ increased with an increasing initial concentration of diuron. This fact can be related to a faster consumption of photogenerated hydroxyl radicals by higher concentrated organic molecules. Consequently, the photostationary concentration of hydroxyl radicals decreased. It corresponds to the observed decrease in the formal rate constants. On the other hand, lower concentration of hydroxyl radicals reduces a probability of the recombination of hydroxyl radicals with electrons trapped on surface of the Q-TiO$_2$ particles. This could cause the observed fall in quantum yields with decreasing concentration of diuron.

The values in Table 3 also show that the reaction rate of diuron degradation decreased with increasing acidity of the solution. An analogous dependence was also described for degradation of other compounds [13]. In the case of 4-chlorophenol, the reaction rate increased with decreasing acidity in the range between pH 1 and 6. However, the reaction rate did not change for pH between 6 and 11. In our experiments, the pH values varied only from 1.9 (0.02 mol l^{-1} HClO$_4$) to 2.7 (0.002 mol l^{-1} HClO$_4$). Higher pH values could not be used due to problems with coagulation of the colloidal particles. The observed decrease of the degradation rate of diuron with the decreasing pH values is probably connected with redox properties of the Q-TiO$_2$ particles. The surface of these particles is protonated in acid solutions. During the acidification, a total positive charge of the semiconductor particles is increasing due to higher extent of the surface protonation and thus the redox potentials of both positive holes and negative electrons are shifting toward to more positive values. The more positive potential of separated electrons causes a retardation of their interfacial transfer to dioxygen. The photostationary concentration of the separated electrons in semiconductor particles is then higher and therefore a probability of their recombination with newly photogenerated positive holes increases. Due to the higher recombination probability the formation of hydroxyl radicals is slower and their photostationary concentration decreases. In the consequence, the formal rate constants as well as quantum yields decrease with increasing acidity.

The reaction rate of diuron degradation was also affected by the intensity of irradiation light. Not surprisingly the formal rate constants were increasing with the number of used lamps. In the contrary, lower quantum yields of the diuron degradation would be expected for higher light intensities. A rate of the recombination of positive holes with the electrons should increase with increasing light intensity more progressively than the rates of charge transfer reaction [14]. However, the measured quantum yields scattered. It was most probably caused by experimental errors of the actinometry [15]. For actinometric measurements, equal values of absorbance at the irradiation wavelength of 365 nm had to be adjusted for both colloidal solution and actinometer. However, the used lamps emitted, besides the main irradiation

Table 3
Formal rate constants (a_0) and quantum yields (Φ) for disappearance of diuron under various initial conditions

Number of lamps	c_D (10^{-4} mol l^{-1})	c_{TiO_2} (mol l^{-1})	c_{HClO_4} (mol l^{-1})	a_0 (s^{-1})	Φ (%)
3	5×10^{-4}	10^{-3}	2×10^{-2}	1.19×10^{-3}	0.73
2	5×10^{-4}	10^{-3}	2×10^{-2}	8.33×10^{-4}	1.24
1	5×10^{-4}	10^{-3}	2×10^{-2}	4.93×10^{-4}	1.04
1	7.5×10^{-4}	10^{-3}	2×10^{-2}	3.38×10^{-4}	1.07
1	2.5×10^{-4}	10^{-3}	2×10^{-2}	9.27×10^{-4}	0.982
1	5×10^{-4}	10^{-3}	10^{-2}	5.13×10^{-4}	1.09
1	5×10^{-4}	10^{-3}	2×10^{-3}	7.94×10^{-4}	1.68
1	5×10^{-4}	3.33×10^{-4}	2×10^{-2}	5.62×10^{-4}	1.16
1	5×10^{-4}	10^{-4}	2×10^{-2}	3.21×10^{-4}	0.82

wavelength of 365 nm, also partly at 310 nm (the mercury line) that could be a source of an inaccuracy.

In the case of dependence of the diuron degradation rate on the concentration of colloidal particles it is possible to observe an increase in the formal rate constant and quantum yield for the concentration drop from 10^{-3} to 3.33×10^{-4} mol l^{-1}. However, a next concentration lowering led to a decrease of both values. The explanation of these dependences is not simple. The walls of the tube photoreactor were covered by an aluminum foil to ensure multiple reflections and thus a better utilization of the irradiated light. Some drop in concentration of the Q-TiO$_2$ particles and thus decreased absorbance of the colloidal solution could actually cause a more homogeneous light absorption inside the reaction volume. It implies an optimal concentration of colloidal particles in the photoreactor that enables a most efficient photodegradation course. In our device, this optimal value of the Q-TiO$_2$ concentration was probably close to 3.33×10^{-4} mol l^{-1}.

3.2.2. Kinetic model

On the basis of the reaction pathways of the photocatalytic degradation of diuron (Fig. 2), a corresponding kinetic scheme consisting of parallel consecutive reactions of the first-order kinetics was proposed in Fig. 4. A letter **D** means diuron and all roman numbers were assigned to the particular degradation intermediates according to Table 1. The solid arrows represent transformations between the identified components; the dashed arrows designate reactions to unknown products. The symbols placed above the arrows indicate corresponding formal rate constants of the first-order kinetics. The letter d means a rate constant of the photocatalytic transformation; the letter k is assigned to the rate constants of thermal reactions. The letter a is used as an overall rate constant summing the contributions of all transformations of the particular compound.

How it was already discussed, certain simplifications concerning the observed pseudomonomolecularity were assumed. Extinction coefficients for diuron and its degradation intermediates **I** and **III** were found to be almost equal. Therefore, the same values were assumed for the other derivatives given in Table 1. The structure of these derivatives differs only on the aliphatic side chain and thus the benzene ring as a chromophore is not significantly affected.
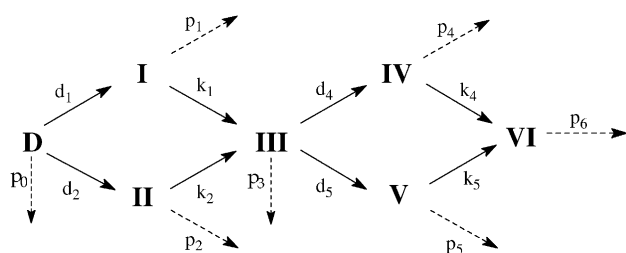
Based on the kinetic scheme shown in Fig. 3, the following set of differential equations can be formulated:

$$-\frac{d[\mathbf{D}]}{dt} = (d_1 + d_2 + p_0)[\mathbf{D}] = a_0[\mathbf{D}] \tag{7}$$

$$\frac{d[\mathbf{I}]}{dt} = d_1[\mathbf{D}] - (k_1 + p_1)[\mathbf{I}] = d_1[\mathbf{D}] - a_1[\mathbf{I}] \tag{8}$$

$$\frac{d[\mathbf{II}]}{dt} = d_2[\mathbf{D}] - (k_2 + p_2)[\mathbf{II}] = d_2[\mathbf{D}] - a_2[\mathbf{II}] \tag{9}$$

$$\frac{d[\mathbf{III}]}{dt} = k_1[\mathbf{I}] + k_2[\mathbf{II}] - (d_4 + d_5 + p_3)[\mathbf{III}]$$
$$= k_1[\mathbf{I}] + k_2[\mathbf{II}] - a_3[\mathbf{III}] \tag{10}$$

$$\frac{d[\mathbf{IV}]}{dt} = d_4[\mathbf{III}] - (k_4 + p_4)[\mathbf{IV}] = d_4[\mathbf{III}] - a_4[\mathbf{IV}] \tag{11}$$

$$\frac{d[\mathbf{V}]}{dt} = d_5[\mathbf{III}] - (k_5 + p_5)[\mathbf{V}] = d_5[\mathbf{III}] - a_5[\mathbf{V}] \tag{12}$$

$$\frac{d[\mathbf{VI}]}{dt} = k_4[\mathbf{IV}] + k_5[\mathbf{V}] - a_6[\mathbf{VI}], \quad a_6 = p_6 \tag{13}$$

The integration of these equations gave an analytical solution. The corresponding formulas for concentrations of diuron and its particular degradation intermediates as functions of time are too long to be introduced in an appendix. Nevertheless, the first author will provide them on request. They were used to fit the experimental kinetic dependences and to estimate the values of the formal rate constants as optimized parameters.

3.2.2.1. Thermal reactions of products **I** and **II**.

It was observed that the primary degradation intermediates **I** and **II** underwent the thermal transformations giving the same product, the secondary degradation intermediate **III**. The corresponding rate constants were determined for two temperatures (8 and 20 °C) and three different concentrations of perchloric acid (0.2, 0.01, 0.002 mol l^{-1}). The results are summarized in Table 4.

Table 4 shows that the reaction rates increased with increasing both temperature and acidity of the solution. The thermal decomposition of substance **I** ran slower than the hydrolysis of compound **II**. The latter processes did not almost take place at the lowest concentration of perchloric acid

Fig. 4. The kinetic scheme of the photocatalytic transformations of diuron in aqueous colloidal solutions of Q-TiO$_2$ particles.

Table 4
First-order rate constants of thermal transformations of compounds **I** and **II**

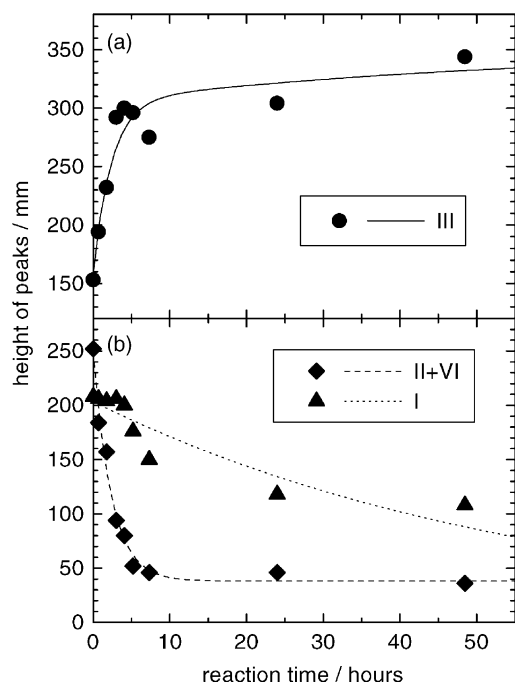| c_{HClO_4} (mol l^{-1})	Temperature (°C)	k_1 (s^{-1})	k_2 (s^{-1})
0.002	8	5.65×10^{-7}	3.29×10^{-6}
0.002	20	1.76×10^{-6}	4.62×10^{-6}
0.01	8	2.47×10^{-6}	4.48×10^{-5}
0.01	20	7.62×10^{-6}	6.29×10^{-5}
0.02	8	4.79×10^{-6}	1.16×10^{-4}
0.02	20	1.49×10^{-5}	1.63×10^{-4}

Fig. 5. The experimental points and fitted kinetic curves for the thermal transformations of degradation intermediates **I** and **II** and formation of corresponding product **III**. Experimental conditions: 5×10^{-5} mol l^{-1} diuron, 2×10^{-2} mol l^{-1} HClO$_4$, 10^{-3} mol l^{-1} Q-TiO$_2$, temperature 20 °C.
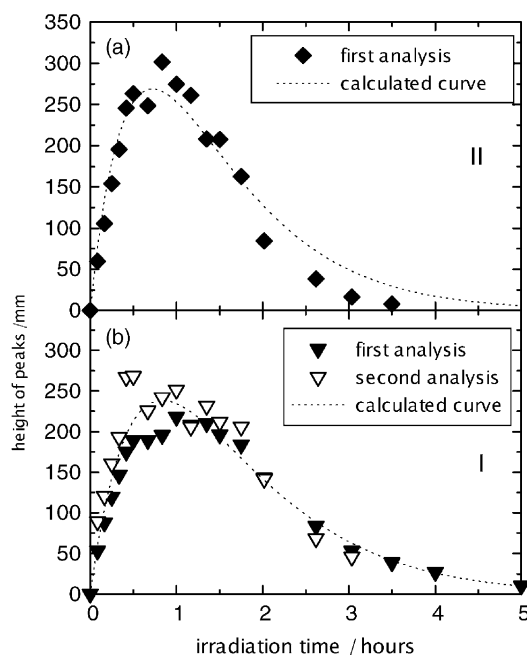

Fig. 6. The extrapolated experimental points and corresponding theoretical fits for the photocatalytic transformations of primary intermediates **I** and **II**. Experimental conditions: 5×10^{-5} mol l^{-1} diuron, 2×10^{-2} mol l^{-1} HClO$_4$, 10^{-3} mol l^{-1} Q-TiO$_2$, temperature 20 °C, one lamp.

(0.002 mol l^{-1}). The Arrhenius activation energy was calculated based on two measurements at temperatures of 8 and 20 °C for the most acidic solution (0.02 mol l^{-1}). The found values were 64.9 kJ mol^{-1} for **I** and 19.3 kJ mol^{-1} for **II**.

An example of experimental time dependences together with corresponding fits of the first-order for the thermal transformations of compounds **I** and **II** to **III** are shown in Fig. 5. It was observed that the chromatographic peak assigned to the primary intermediate **II** did not fully disappear. On the other hand, it was found that a residual peak of the quarternary degradation product **VI** stayed at the same retention time after the compound **II** had been completely transformed to the secondary product **III**.

3.2.3. Use of the kinetic model

The kinetic model described above was applied to analyze the reaction course of the photocatalytic degradation of diuron in an aqueous colloidal solution of Q-TiO$_2$ particles, containing the highest used concentration of perchloric acid. The reaction mixture (70 ml) containing 5×10^{-5} mol l^{-1} of diuron, 2×10^{-2} mol l^{-1} of HClO$_4$, and 10^{-4} mol·l^{-1} of Q-TiO$_2$ was placed into the tube photoreactor. The mixture was magnetically stirred and irradiated by only one lamp. The temperature was kept at 20 °C and thus the thermal reactions of intermediates I and II could not be neglected. Under these conditions, diuron was completely transformed within 4 h and the primary intermediates **I** and **II** reached their maximum concentrations after 40 min of irradiation. The samples (1 ml) taken from the photoreactor

during the course of the whole experiment were kept at 8 °C. A first set of the chromatographic analyses was carried out shortly after taking the samples from the photoreactor and repeated measurements were performed 2 days later. It enables to differentiate the primary intermediate **II** from the quarternary product **VI**. Due to their coincidence in the chromatograms, they could be distinguished only on the base of their different thermal reactivity. Because of the hydrolytic reaction of the compound **II**, only the substance **VI** appeared in the chromatograms after 2 days.

The time profiles of the primary intermediates **I** and **II** are depicted in Fig. 6. The content of the primary product **II** in the time of taking the sample was calculated assuming the first-order kinetics of its thermal reaction with the rate constant k_2 (Table 4) determined for 8 °C (probes were stored in a refrigerator) after the contribution of the quarternary product **VI** obtained from the second HPLC analyses had been subtracted.

The same principle was applied for the other primary intermediate **I**. In this case, there was no coincidence with any other peak in HPLC chromatograms. Both analyses performed within 2 days were used to extrapolate initial values in the times of taking samples. The results are represented in Fig. 6b as open and bold symbols. It can be seen that these two data sets are in a good agreement and do not show any systematic differences. Small variations are within the interval of experimental error. The extrapolated experimental points in Fig. 6a and b were completed with the theoretical kinetic curves. The curves were computed
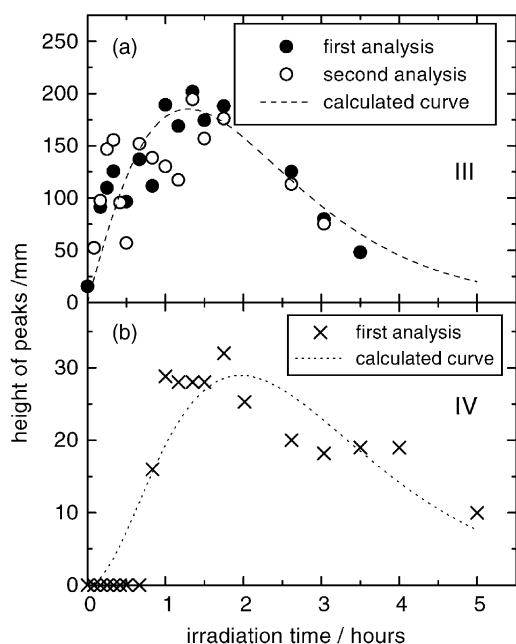
Fig. 7. The extrapolated experimental points and corresponding kinetic curves of the secondary intermediate **III** and tertiary product **IV**. Experimental conditions: $5 \times 10^{-5} \, mol \, l^{-1}$ diuron, $2 \times 10^{-2} \, mol \, l^{-1}$ HClO$_4$, $10^{-3} \, mol \, l^{-1}$ Q-TiO$_2$, temperature 20 °C, one lamp.

Fig. 8. The estimated rate constants (in $10^{-5} \, s^{-1}$) for the photocatalytic transformations of diuron and its degradation intermediates.

by non-linear regression using integration formulas derived from the differential equations (8) and (9). In these cases, thermal rate constants k_1 and k_2 for 20 °C were used (temperature of the photocatalytic experiment). Other rate constants were obtained from the regression procedure as optimized parameters (Fig. 8).

The secondary intermediate **III** was mainly formed by acid catalyzed thermal reactions, i.e. decomposition of **I** and hydrolysis of **II**. The heights of chromatographic peaks of **III** were extrapolated to the time point of taking samples for both sets of measurements using k_1 and k_2 at 8 °C (Fig. 7a). The corresponding theoretical kinetic curve according to integrated equation (10) employing k_1 and k_2 at 20 °C is added to this graph.

An application in the proposed kinetic model to the tertiary intermediates **IV** and **V** and quarternary product **VI** was formally possible (e.g. Fig. 7b) but did not lead to satisfactory results concerning the rate constants. Too low concentrations of these components of the reaction mixture that disabled their reproducible determination by HPLC was the main reason of it. Therefore, we decided to prepare the compound **III** synthetically and perform a separate kinetic study of its photocatalytic degradation in colloidal solution of Q-TiO$_2$ particles. The results of this study will be described in another paper [16].

All rate constants estimated on the basis of the proposed kinetic model are graphically summarized in Fig. 8. Similar values of the overall rate constants for the photocatalytic degradation of diuron as well as its particular intermediates, $a_0 = 32.2 \approx a_1 = 32.8 \approx a_2 = 29.7 \approx a_3 = 30.2 \approx a_4 = 28.1$ (numeric values in $10^{-5} \, s^{-1}$), indicate that the pho-
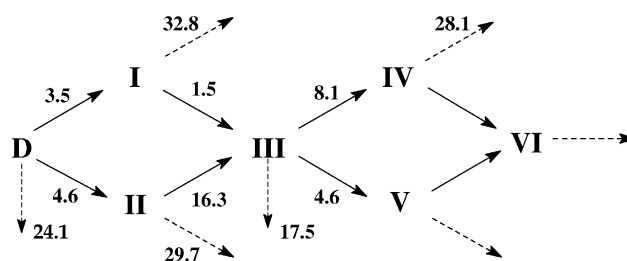
togeneration of hydroxyl radicals followed by OH-attacks on the organic molecules of similar structure run with approximately equal rate constants. This observation confirmed fulfilling of the presumptions concerning the pseudomonomolecularity mentioned above (part 3.2). Similar rate constants of the formation of both primary intermediates **I** and **II** correspond with proposed reaction mechanism assuming the disproportionation of peroxyl radical **R$_1$OO$^\bullet$** (3).

3.3. Electrochemically assisted photocatalytic degradation of diuron

The photocatalytic degradation of diuron that occurred in acetonitrile on polarized TiO$_2$ layers was investigated in detail in dependence on the external voltage. The degradation rate of diuron increased with increasing applied voltage in the range from 0 and +1 V vs. Ag electrode. The next increase of potential up to +1.5 V did not affect the reaction rate yet. A bending of the semiconductor energetic levels on the positively polarized TiO$_2$ electrode led probably to a better separation of photogenerated charge carriers and thus to reduction of their internal recombination. In this consequence, a higher photostationary concentration of positive holes occurred on the illuminated TiO$_2$ surface while electrons moved to the counter electrode. As a result, the degradation of diuron proceeded more effectively. However, the reaction rate at the same applied voltage was several times higher in aqueous solutions than in acetonitrile (Fig. 9). Also the reaction mechanism of these electrochemically assisted photocatalytic degradation processes of diuron was different for these solvents.

While identical intermediates with those of the photocatalytic degradation in aqueous colloidal solutions of Q-TiO$_2$ particles were observed in water, monuron [3-(4-chlorophenyl)-1,1-dimethylurea] and its isomer [3-(3-chlorophenyl)-1,1-dimethylurea] were found as main products in acetonitrile. In the presence of organic solvents, the photogenerated positive hole was probably transferred directly to benzene ring of the diuron molecule yielding corresponding radical cation with the positive charge delocalized over the π-electron system. The lowered number of electrons should reduce the bond order between aromatic carbons and chlorine substituents and thus the C–Cl bonds could split. The formed transients carrying carbene structure
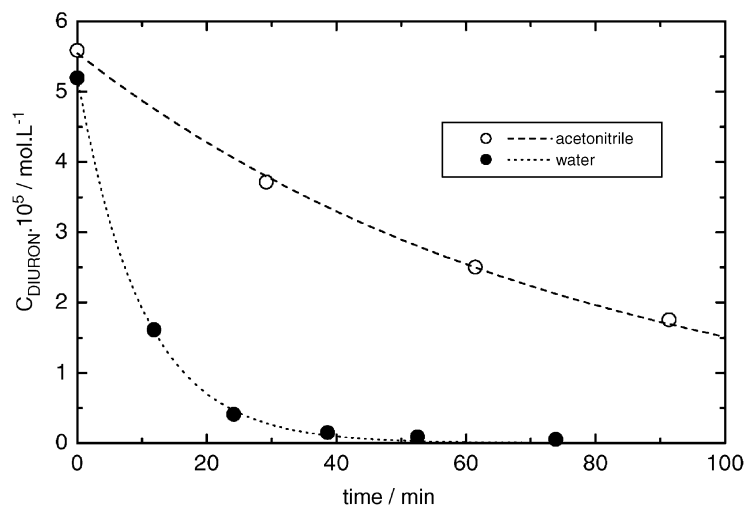
Fig. 9. Electrochemically assisted photocatalytic degradation of diuron on illuminated TiO$_2$ electrode, polarized applying an external voltage of $+1$ V vs. Ag, in both water and acetonitrile. The initial concentration of diuron was 5×10^{-5} mol l^{-1}.

on aromatic carbon [17] react in acetonitrile producing monuron or its isomer. An analogous reaction pathway was observed during direct photolysis of diuron in water containing small amounts of organic solvents, e.g. methanol [18,19]. Monuron and its isomer could also partly result from the reduction of diuron on the counter electrode [21].

4. Conclusions

Only transformations on the side aliphatic chain were observed during the photocatalytic degradation of diuron in aqueous colloidal solutions of Q-TiO$_2$ particles. However, a detailed kinetic analysis showed that only about one-third of diuron molecules were transformed according to this mechanism. The other two-thirds had to undergo other reactions leading to intermediates that were not detectable using HPLC with absorption detection. These reaction pathways were probably initiated by OH-attacks onto benzene ring of diuron and they caused its opening.

There are two different reaction mechanisms of an electrochemically assisted photocatalytic degradation of diuron on TiO$_2$ layers for aqueous and non-aqueous solvents. However, neither one mechanism corresponds to the processes observed for an oxidative electrochemical degradation of diuron on classic platinum electrode [20] where a complete blockage of the electrode surface took place. The electrode surface was blocked due to formation of dimeric products. In our case, no electrode blockage occurred in either acetonitrile or water and therefore the application of illuminated TiO$_2$ electrodes can be a promising photoelectrochemical method for removing of phenylurea pollutants.

References

[1] T.R. Roberts (Ed.), Methabolic Pathways of Agrochemicals. Part 1. Herbicides and Plant Growth Regulators, The Royal Society of Chemistry, Bookcraft (Bath) Ltd., Cambridge 1998, p. 705.
[2] J. Jirkovský, V. Faure, P. Boule, Pestic. Sci. 50 (1997) 42.
[3] P.H. Mazzochi, M.P. Rao, J. Agric. Food Chem. 20 (1972) 957.
[4] P. Mazellier, J. Jirkovský, M. Bolte, Pestic. Sci. 49 (1996) 259.
[5] H. Krýsová, J. Krýsa, K. Macounová, J. Jirkovský, J. Chem. Technol. Biotechnol. 72 (1998) 169.
[6] M.A. Fox, M.T. Dulay, Chem. Rev. 93 (1993) 341.
[7] Y. Wang, N. Herron, J. Phys. Chem. 95 (1991) 525.
[8] A. Henglein, Top. Curr. Chem. 143 (1988) 113.
[9] C. Kormann, D.V. Bahnemann, M.R. Hoffmann, J. Phys. Chem. 92 (1988) 5196.
[10] M. Krejčík, M. Daněk, F. Hartl, J. Electroanal. Chem. 317 (1991) 179.
[11] L. Kavan, B. O'Regan, A. Kay, M. Grätzel, J. Electroanal. Chem. 346 (1993) 291.
[12] B. O'Regan, M. Grätzel, Nature 353 (1991) 737.
[13] F. Sabin, T. Türk, A. Vogler, J. Photochem. Photobiol. A 63 (1992) 99.
[14] M.R. Hofmann, S.T. Martin, W. Choj, D.V. Bahnemann, Chem. Rev. 95 (1995) 69.
[15] J.F. Rabek, Experimental Methods in Photochemistry and Photophysics, Wiley, Chichester, UK, 1982, p. 944.
[16] K. Macounová, L. Hykrdová, J. Urban, J. Jirkovský, G. Grabner, in preparation.
[17] G. Grabner, C. Richard, G. Köhler, J. Am. Chem. Soc. 116 (1994) 11470.
[18] P.H. Mazzochi, M.P. Rao, J. Agric. Food Chem. 20 (1972) 957.
[19] G. Durand, D. Barceló, J. Albaiges, M. Mansoor, Toxicol. Environ. Chem. 32 (1991) 55.
[20] K. Macounová, J. Klíma, C. Bernard, C. Degrand, J. Electroanal. Chem. 457 (1998) 141.
[21] M.R. Rifi, Electrochemical reduction of organic halides. In Organic Electrochemistry, M.M. Baizer (Ed.), M. Dekker Inc., New York, 1973.